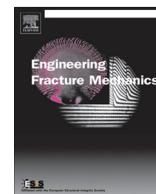




ELSEVIER

Contents lists available at ScienceDirect

Engineering Fracture Mechanics

journal homepage: www.elsevier.com/locate/engfracmechEstimation of C^* including the effect of threshold stressHuan Sheng Lai^a, Shu Feng Xu^a, Kang Lin Liu^a, Chunmei Bai^{b,*}, Ling Zhu Gong^a, Jin-quan Guo^c^a School of Chemical Engineering, Fuzhou University, Fuzhou, Fujian 350-116, China^b College of Civil Engineering, Fuzhou University, Fuzhou, Fujian 350116, China^c School of Mechanical Engineering and Automation, Fuzhou University, Fuzhou 350-116, China

ARTICLE INFO

Article history:

Received 24 June 2017

Received in revised form 13 December 2017

Accepted 20 December 2017

Available online xxxxx

Keywords:

Threshold stress

Estimation method of C^*

GE/EPRI method

Reference stress method

ABSTRACT

In some alloys such as 9%Cr heat resistant steels and magnesium alloys, the creep constitutive equation of the power-law requires a term of threshold stress due to the presence of second phase particles. It is necessary to establish an estimation method of C^* for such alloys to predict the life of their components. In this paper, the General Electric/Electric Power Research Institute (GE/EPRI) method and the reference stress method were modified to estimate C^* for power-law creep materials with threshold stress. The finite element method was used to verify the accuracy of the modified methods. The accuracy of the calculation equation of C^* in the American Society for Testing Materials (ASTM) E 1457 was also assessed. The results indicated that the modified GE/EPRI method was sufficiently exact as an engineering method. h_1 was slightly affected by the applied load and significantly affected by the threshold stress. The accuracy of the modified reference stress method increased with increased applied load and was within $\pm 40\%$. The accuracy of the calculation equation of C^* in ASTM E 1457 was not affected by the threshold stress and the equation could be directly used for power-law creep materials with threshold stress.

© 2018 Elsevier Ltd. All rights reserved.

1. Introduction

C^* is one of the parameters used for characterizing the creep crack growth and the stress field at the crack tip region. Accurate estimation of C^* plays an important role in the analysis of fracture mechanics and lifetime prediction for structures at elevated temperatures. Many studies have been conducted to research estimation methods of C^* . The General Electric/Electric Power Research Institute (GE/EPRI) method is widely used to estimate C^* for homogeneous materials [1,2]. The reference stress method is another widely used method for estimating C^* [3,4]. Based on the reference stress method, Xuan [5] proposed a method to estimate C^* for mismatched weld creep cracks and Kim [6,7] proposed an enhanced reference stress method to estimate C^* . Other methods have also been proposed to estimate C^* for mismatched weld creep cracks [8,9] in addition to cracks in thin T-sections [10] and annular discs [11]. Further, the calculation equation of C^* in the American Society for Testing Materials (ASTM) E 1457 was modified for mismatched weld creep cracks by Xuan [12]. However, there has been no research on the estimation of C^* for materials with power-law creep constitutive equations that include a term of threshold stress. Since threshold stress exists in some alloys due to the presence of second-phase or nanometer-sized particles, such as dispersion hardened alloys [13–16] and nanocomposites [17,18], it is necessary to establish estimation methods of C^* with the effect of threshold stress included.

* Corresponding author.

E-mail address: baichunmei2005@163.com (C. Bai).

Nomenclature

A	power-law creep coefficient
a	crack length
B	specimen thickness
C^*	a path-independent C-integral defined under the extensive steady state creep stage
C_{EPRI}^*	C^* estimated by the GE/EPRI method
C_{FEM}^*	C^* calculated by finite element method
C_{REF}^*	C^* estimated by reference stress method
C_{Vc}^*	C^* calculated by the equation in ASTM E 1457
E	Young's modulus
e_{EPRI}	$e_{EPRI} = 100\% \times (C_{EPRI}^* - C_{FEM}^*) / C_{FEM}^*$
e_{REF}	$e_{REF} = 100\% \times (C_{REF}^* - C_{FEM}^*) / C_{FEM}^*$
e_{Vc}	$e_{Vc} = 100\% \times (C_{Vc}^* - C_{FEM}^*) / C_{FEM}^*$
$\dot{\epsilon}$	creep strain rate
$\dot{\epsilon}_{ref}$	creep strain rate at σ_{ref}
$h_1(a/W, n)$	dimensionless function of a/W and n
$h_1(a/W, n, \sigma_0)$	dimensionless function of a/W , n , and σ_0
n	power-law creep exponent
η_1	a dimensionless function dependent on a and W
P	applied load
P_L	plastic limit load
$(\dot{V}_c)_{SS}$	load line deflection rate under the extensive steady state creep stage
W	specimen width
ν	Poisson's ratio
$\sigma, \dot{\sigma}, \sigma_0$	stress, stress rate, and threshold stress, respectively
$\sigma_{0.2}, \sigma_{ref}$	0.2% proof stress or the stress at 0.2% inelastic strain, and reference stress, respectively

In this paper, the GE/EPRI method and the reference stress method were implemented first, then modified to estimate C^* for power-law creep materials with threshold stress. The finite element method was then used to verify and assess the accuracy of the modified methods. The accuracy of the calculation equation of C^* in ASTM E 1457 was also investigated.

2. Estimation method of C^*

When the primary creep and tertiary creep stages are ignored, the steady state creep stage with elastic properties is usually described by a constitutive equation of elastic plus power-law creep [9]:

$$\dot{\epsilon} = \frac{\dot{\sigma}}{E} + A\sigma^n \quad (1)$$

where A and n are the creep coefficient and exponent, respectively; E is the elastic modulus; $\dot{\epsilon}$ is the creep strain rate; σ and $\dot{\sigma}$ are the stress and stress rate, respectively. Under the extensive steady state creep stage, C^* for compact tension (CT) specimens can be estimated using the GE/EPRI method (denoted as C_{EPRI}^*):

$$C_{EPRI}^* = A(W - a)h_1(a/W, n) \left(\frac{P}{1.455\eta_1 B(W - a)} \right)^{n+1} \quad (2)$$

where W is the specimen width, B is the specimen thickness, a is the crack length, P is the applied load, η_1 is the dimensionless function of a and W , and h_1 is the dimensionless function of a/W and n [19]. C^* can also be estimated using the reference stress method (denoted as C_{REF}^*) [20]:

$$C_{REF}^* = \left(\frac{K^2}{E'} \right) \frac{E\dot{\epsilon}_{ref}}{\sigma_{ref}} \quad (3)$$

where K is the stress intensity factor, σ_{ref} is the reference stress, $\dot{\epsilon}_{ref}$ is the creep strain rate at σ_{ref} ($\dot{\epsilon}_{ref} = A\sigma_{ref}^n$), $E' = E$ for plane stress, and $E' = E/(1 - \nu^2)$ for plane strain. In addition, based on the ASTM E 1457 standard [21], C^* for CT specimens can be calculated with the following equation using the load line displacement rate (denoted as C_{Vc}^*):

$$C_{Vc}^* = \frac{P(\dot{V}_c)_{SS}}{BW} \left(\frac{2}{(1 - a/W)} + 0.522 \right) \frac{n}{n + 1} \quad (4)$$

where $(\dot{V}_c)_{SS}$ is the load line deflection rate under the extensive steady state creep stage.

Power-law creep materials with threshold stress are characterized by [15,22]:

$$\dot{\epsilon} = A(\sigma - \sigma_0)^n \quad (5)$$

where σ_0 is the threshold stress, which decreases with increased temperature [15,23]. Note that the value of n in Eq. (1) can be affected by the testing temperature, but the value in Eq. (5) is independent of the testing temperature. When σ_0 is equal to 0, Eq. (5) becomes the power-law creep model for $\dot{\epsilon} = A\sigma^n$. The elastic-creep model for power-law creep materials with threshold stress is hence assumed to be:

$$\dot{\epsilon} = \frac{\dot{\sigma}}{E} + A(\sigma - \sigma_0)^n \quad (6)$$

In order to estimate C^* for the CT specimens of power-law creep materials with threshold stress, Eqs. (2) and (3) are modified in the following manner:

$$C_{EPRI}^* = A(W - a)h_1(a/W, n) \left(\frac{P}{1.455\eta_1 B(W - a)} - \sigma_0 \right)^{n+1} \quad (7)$$

$$C_{ref}^* = \left(\frac{K^2}{E'} \right) \frac{E\dot{\epsilon}_{ref}}{\sigma_{ref} - \sigma_0} \quad (8)$$

where $\dot{\epsilon}_{ref} = A(\sigma_{ref} - \sigma_0)^n$. When $\sigma_0 = 0$ MPa, Eq. (7) becomes Eq. (2) and Eq. (8) becomes Eq. (3). Since C^* is a positive value and n is a positive real number, σ_0 has to be smaller than $P/[1.455\eta_1 B(W - a)]$ in Eq. (7) and σ_{ref} in Eq. (8). The accuracy of Eqs. (7) and (8) was validated using the finite element method and was discussed in the following sections. Eq. (4) was also used to calculate C^* for power-law creep materials with threshold stress, and its accuracy was analyzed as well.

3. Finite element analysis

The dimensions of a standard 0.5T-CT specimen were used to model the specimen in the general finite element software Abaqus. This means that the W of the specimen was equal to 25.4 mm [24]. The crack ratio (a/W) was 0.5. Only half of the specimen was modeled in two dimensions, with the crack plane used as a symmetry plane. The finite element model employed is shown in Fig. 1. The crack-tip region had finer mesh than the other regions, as shown in Fig. 1(b). In the model, 4093 elements were used with 12,539 nodes. The symmetry boundary condition was applied to the uncracked ligament, as shown in Fig. 1(a); the crack tip was initially sharp. A rigid pin (the green circle) was passed through to the pinhole of the specimen, and load was directly applied to the loading point of the rigid pin, as shown in Fig. 1(a). Therefore, the load was applied to the specimen by the rigid pin, as in actual tests. The applied loads of P for simulated cases 1–12 are shown in Table 1. The surface friction coefficient between the rigid pin and the pinhole was fixed at 0.3 [25–27]. The element type used was CPE8R, which is an eight node, plane strain, and reduced integration element. $(\dot{V}_c)_{SS}$ was obtained at the measurement point for load line deflection, as shown in Fig. 1(a). C^* was calculated on the third contour surrounding the crack tip and denoted as C_{FEM}^* . In this paper, C_{FEM}^* was considered the exact C^* . C^* obtained from other methods was compared with C_{FEM}^* to judge their accuracy.

The material constitutive equation is shown in Eq. (6). The power-law creep behavior with threshold stress, as shown in Eq. (5), was achieved through the use of the CREEP subroutine. Simulated cases 1–12 had the same elastic properties with $E = 175$ GPa and $\nu = 0.3$, as well as the same A and n [15], but had different σ_0 and P , as shown in Table 1. Therefore, cases 1–12 had the same materials properties with the exception of different values for σ_0 and P .

4. Accuracy of the modified methods and discussion

The estimated and simulated C^* values are shown in Table 1 for cases 1–12, where e_{EPRI} , e_{REF} , and e_{VC} are the errors between C_{FEM}^* and C_{EPRI}^* , C_{FEM}^* and C_{REF}^* , and C_{FEM}^* and C_{VC}^* , respectively, defined as follows:

$$e_{EPRI} = \frac{C_{EPRI}^* - C_{FEM}^*}{C_{FEM}^*} \times 100\% \quad (9)$$

$$e_{REF} = \frac{C_{REF}^* - C_{FEM}^*}{C_{FEM}^*} \times 100\% \quad (10)$$

$$e_{VC} = \frac{C_{VC}^* - C_{FEM}^*}{C_{FEM}^*} \times 100\% \quad (11)$$

The accuracy of the modified GE/EPRI method in Eq. (7) is shown in Fig. 2, where h_1 in Eq. (7) was equal to 0.919 for cases 1–12 with $a/W = 0.5$ and $n = 5$ [19]. Cases 1–6 had the same P , but σ_0 increased by 30 MPa in each case from 0 MPa to 150 MPa, respectively. As demonstrated by the stars in Fig. 2, the error increased with increasing σ_0 for cases 1–6. Especially, the

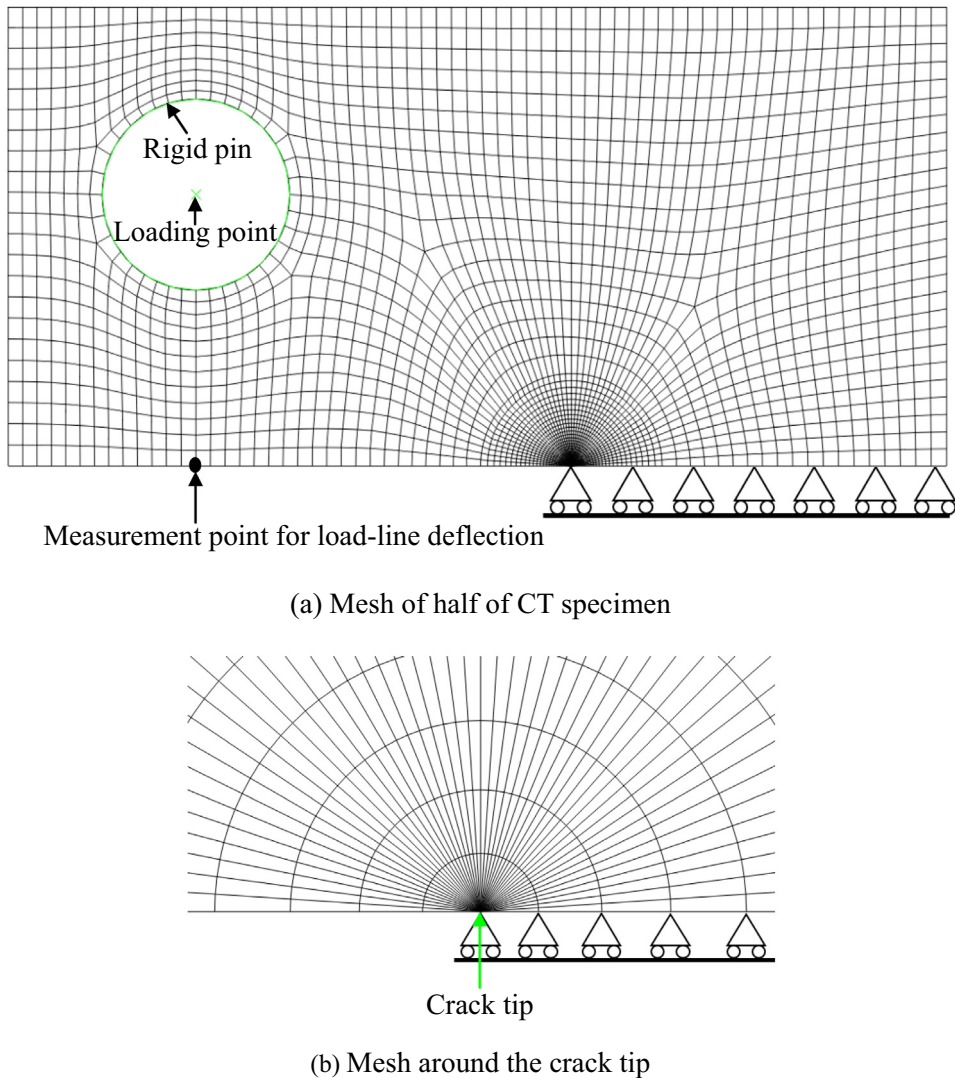


Fig. 1. Finite element model of the 0.5 T-CT specimen ($a/W = 0.5$).

error increased rapidly from 206% to 560% when σ_0 increased from 120 MPa to 150 MPa. Half of $P/[1.455\eta_1 B(W - a)]$ in Eq. (7) with $P = 9000$ N was 117.44 MPa. Thus, the error would increase rapidly when σ_0 was larger than half of $P/[1.455\eta_1 B(W - a)]$. The error decreased with increased P as demonstrated by the solid circles in Fig. 2 for cases 4, 10, 11, and 12. These cases had the same material properties with $\sigma_0 = 90$ MPa, but P increased from 9000 N to 12,000 N, respectively. It should be noted that the accuracy of the GE/EPRI method or Eq. (2) was almost unaffected by P . This was because the error barely changed under different P values for cases 1, 7, 8, and 9, which had $\sigma_0 = 0$ MPa and P values that increased from 9000 N to 12,000 N, respectively.

The above analysis indicated that the accuracy of Eq. (7) was affected by σ_0 and P , but the effect of P was much smaller than that of σ_0 . The slight effect of P and the large effect of σ_0 on the accuracy of Eq. (7) was induced by the parameter h_1 . This was because the value of h_1 was obtained from previous finite element analyses without σ_0 or with $\sigma_0 = 0$ MPa [19]. When $\sigma_0 = 0$ MPa, Eq. (7) became Eq. (2). Consequently, the accuracy of the GE/EPRI method or Eq. (2) could not be affected by creep and geometry parameters and was nearly unaffected by P , though it was affected by h_1 . Therefore, the effect of P on the accuracy of Eq. (7) was possibly induced by σ_0 and this effect could be estimated by modifying the value of h_1 . However, the effect of P on the accuracy of Eq. (7) or h_1 was much smaller than that of σ_0 . This effect could therefore be ignored. This meant that h_1 was affected by a/W , n , and σ_0 , and the creep and geometry parameters of A , n , a , W , and η_1 could not affect the accuracy of Eq. (7). In order to verify that the creep and geometry parameters could not affect the accuracy of Eq. (7), another 6 cases (A1–A6) were simulated as shown in Table 2. Cases A1–A6 had the same elastic properties and geometry parameters as cases 1–6. Comparison of Table 1 with Table 2 showed that cases 1 and A1, cases 2 and A2, cases 3 and A3,

Table 1
Threshold stress, applied load, and C^* for cases 1–12.

Case	A (MPa ⁻ⁿ /h)	n	σ_0 (MPa)	P (KN)	C_{FEM}^* (MPa-m/h)	C_{EPRI}^* (MPa-m/h)	C_{REF}^* (MPa-m/h)	C_{Vc}^* (MPa-m/h)	e_{EPRI} (%)	e_{REF} (%)	e_{Vc} (%)
1	1.26×10^{-17}	5	0*	9	1.70E-5	2.57E-5	1.70E-5	1.80E-5	51	0	6
2	1.26×10^{-17}	5	30	9	6.96E-6	1.14E-5	8.00E-6	7.16E-6	64	15	3
3	1.26×10^{-17}	5	60	9	2.45E-6	4.45E-6	3.16E-6	2.40E-6	81	29	-2
4	1.26×10^{-17}	5	90	9	6.66E-7	1.45E-6	9.39E-7	6.27E-7	118	41	-6
5	1.26×10^{-17}	5	120	9	1.20E-7	3.68E-7	1.63E-7	1.10E-7	206	36	-8
6	1.26×10^{-17}	5	150	9	9.33E-9	6.16E-8	6.79E-9	8.80E-9	560	-27	-6
7	1.26×10^{-17}	5	0	10	3.20E-5	4.84E-5	3.20E-5	3.05E-5	51	0	-5
8	1.26×10^{-17}	5	0	11	5.69E-5	8.58E-5	5.69E-5	6.03E-5	51	0	6
9	1.26×10^{-17}	5	0	12	9.61E-5	1.45E-4	9.61E-5	1.02E-4	50	0	6
10	1.26×10^{-17}	5	90	10	1.92E-6	3.91E-6	2.65E-6	1.83E-6	104	38	-5
11	1.26×10^{-17}	5	90	11	4.73E-6	9.15E-6	6.39E-6	4.54E-6	93	35	-4
12	1.26×10^{-17}	5	90	12	1.03E-05	1.93E-05	1.37E-5	1.00E-5	87	33	-3

* Note: Case has no threshold stress when $\sigma_0 = 0$ MPa.

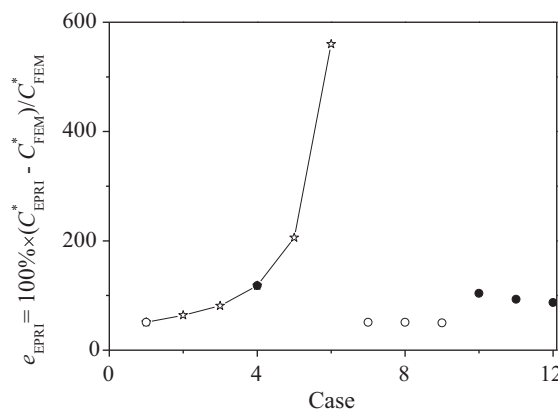


Fig. 2. Error of the modified GE/EPRI method for cases 1–12.

Table 2
Threshold stress, applied load, and C^* for cases A1–A6.

Case	A (MPa ⁻ⁿ /h)	n	σ_0 (MPa)	P (KN)	C_{FEM}^* (MPa-m/h)	C_{EPRI}^* (MPa-m/h)	e_{EPRI} (%)
A1	1.26×10^{-14}	5	0	9	1.70E-2	2.57E-2	51
A2	1.26×10^{-14}	5	30	9	6.96E-3	1.14E-2	64
A3	1.26×10^{-14}	5	60	9	2.45E-3	4.45E-3	81
A4	1.26×10^{-14}	5	90	9	6.66E-4	1.45E-3	118
A5	1.26×10^{-14}	5	120	9	1.20E-4	3.68E-4	206
A6	1.26×10^{-14}	5	150	9	9.33E-5	6.16E-5	560

cases 4 and A4, cases 5 and A5, and cases 6 and A6 had identical n , σ_0 , and P , but different A values. A was 1.26×10^{-17} for cases 1–6 and 1.26×10^{-14} for cases A1–A6. The h_1 value of 0.919 was also used to calculate C_{EPRI}^* for cases A1–A6, because cases A1–A6 had the same value of a/W and n as cases 1–6. As shown in Fig. 3, cases 1 and A1, cases 2 and A2, cases 3 and A3, cases 4 and A4, cases 5 and A5, and cases 6 and A6 had the same error values. Therefore, the accuracy of Eq. (7) was not affected by the creep or geometry parameters but affected by h_1 and Eq. (7) was modified as follows:

$$C_{EPRI}^* = A(W - a)h_1(a/W, n, \sigma_0) \left(\frac{P}{1.455\eta_1 B(W - a)} - \sigma_0 \right)^{n+1} \quad (12)$$

where $h_1(a/W, n, \sigma_0)$ was a dimensionless function of a/W , n , and σ_0 and could be calculated as follows:

$$h_1(a/W, n, \sigma_0) = C_{FEM}^* / \left[A(W - a) \left(\frac{P}{1.455\eta_1 B(W - a)} - \sigma_0 \right)^{n+1} \right] \quad (13)$$

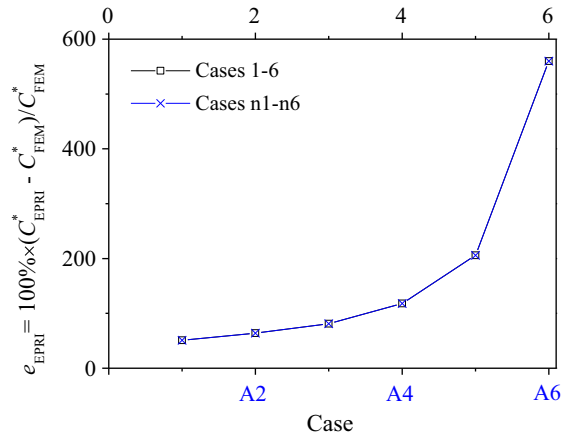


Fig. 3. Error of the modified GE/EPRI method for cases 1–6 and cases A1–A6.

Table 3

$h_1(a/W, n, \sigma_0)$ for cases 1–12 with $a/W = 0.5$ and $n = 5$.

Case	1	2	3	4	5	6	7	8	9	10	11	12
$h_1(a/W, n, \sigma_0)$	0.919	0.849	0.767	0.636	0.454	0.211	0.919	0.923	0.925	0.683	0.719	0.744

Since $h_1(a/W, n)$ was obtained from previous finite element analyses without σ_0 [19] and Eq. (13) indicated that the value of $h_1(a/W, n, \sigma_0)$ was equal to $h_1(a/W, n)$ when $\sigma_0 = 0$ MPa, $h_1(a/W, n)$ was considered $h_1(a/W, n, \sigma_0)$ with $\sigma_0 = 0$ MPa. Therefore, $h_1(a/W, n, \sigma_0)$ was equal to 0.919 for case 1 with $a/W = 0.5$, $n = 5$, and $\sigma_0 = 0$ MPa. The error was 51% for case 1 and this error of 51% was used to calculate $h_1(a/W, n, \sigma_0)$ for cases 2–12 to obtain a conservative value as shown in Table 3, because $h_1(a/W, n, \sigma_0)$ was slightly affected by P . As shown in Table 3, $h_1(a/W, n)$ or $h_1(a/W, n, \sigma_0)$ with $\sigma_0 = 0$ MPa was slightly affected by P , because cases 1, 7, 8, and 9 had no σ_0 and their creep constitutive became the power-law creep model ($\dot{\epsilon} = A\sigma^n$). P effects on $h_1(a/W, n, \sigma_0)$ became slightly larger when σ_0 equaled 90 MPa for cases 4, 10, 11, and 12 and large $h_1(a/W, n, \sigma_0)$ values were obtained under large P values (case 12), as shown in Table 3. Hence, $h_1(a/W, n, \sigma_0)$ should be obtained from a case with large P to ensure a larger or conservative estimated C^* . Consequently, using the modified GE/EPRI method to predict the life of components would lead to a shorter life and safer results. In other words, the modified GE/EPRI method of Eq. (12) is sufficiently exact and conservative as an engineering method when the value of $h_1(a/W, n, \sigma_0)$ is known.

σ_{ref} must be known when the reference stress method is used to estimate C^* . σ_{ref} can be calculated using the plastic limit load, P_L , and the 0.2% proof stress or the stress at 0.2% inelastic strain, $\sigma_{0.2}$, as follows [20]:

$$\sigma_{\text{ref}} = \frac{P}{P_L} \sigma_{0.2} \quad (14)$$

The expression of P_L is shown in the literature for different geometries [19,20]. Since $\sigma_{0.2}$ was not listed in the reference from which the material properties in this paper were obtained [15], σ_{ref} could not be calculated with Eq. (14). However, if C^* is already known, σ_{ref} can be calculated with Eq. (3). Therefore, σ_{ref} was calculated with:

$$\sigma_{\text{ref}} = \left(\frac{K^2}{E'} \right) \frac{E\dot{\epsilon}_c}{C_{\text{REF}}^*} \quad (15)$$

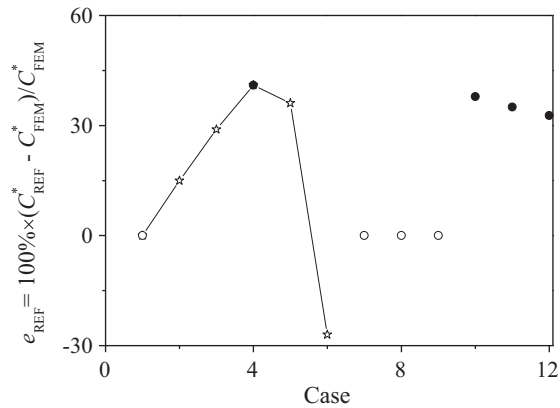
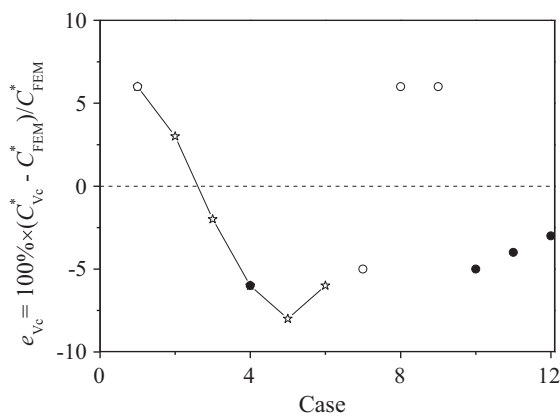
In this paper, σ_{ref} was calculated with Eq. (15) under different P values for cases with $\sigma_0 = 0$, and the modified reference stress method of Eq. (8) was used to estimate C^* for other cases with $\sigma_0 \neq 0$.

In order to calculate σ_{ref} precisely, K and C^* were first calculated using the finite element method for cases 1, 7, 8, and 9 and then σ_{ref} was calculated with Eq. (15). The calculated K and C^* are shown in Table 1 and Table 4 for cases 1, 7, 8, and 9, respectively. The calculated σ_{ref} values are shown in Table 4. As shown in Table 4, σ_{ref} increased with increased P . Since σ_0 was equal to zero in cases 1, 7, 8, and 9, the variation of σ_{ref} was caused by P . It has been demonstrated that σ_{ref} is affected by geometry [20]. Therefore, it can be concluded that σ_{ref} is not only dependent on geometry, but also dependent on P .

Cases 2–5 had the same P and material properties, with the exception of σ_0 . As demonstrated by the stars in Fig. 4 for cases 2–5, the error of the modified reference stress method first increased with increased σ_0 and reached a maximum positive value of 41% for case 4 with $\sigma_0 = 90$ MPa. Afterward, the error decreased with increased σ_0 and reached a value of -27%

Table 4Calculated K and σ_{ref} used finite element method.

Case	1	7	8	9
K (MPa $\sqrt{\text{m}}$)	39.9	44.34	48.78	53.22
σ_{ref} (MPa)	174.69	194.10	213.70	233.23

**Fig. 4.** Error of the modified reference stress method.**Fig. 5.** Error of the calculation equation of C^* in ASTM E 1457.

for case 6 with $\sigma_0 = 150$ MPa. Cases 4, 10, 11, and 12 had the same material properties with different P , which increased by 1000 N in each case from 9000 N to 12,000 N, respectively. The error decreased with increased P as indicated by the solid circles in Fig. 4 for cases 4, 10, 11, and 12. Since $\sigma_{\text{ref}} = 174.69$ MPa and $\sigma_0 = 150$ MPa for case 6, and σ_0 had to be smaller than σ_{ref} in Eq. (8), it could be deduced that the maximum error was possibly a little larger than -27% when σ_0 approached the value of 174.69 MPa for σ_{ref} . Therefore, the accuracy of the modified reference stress method was within $\pm 40\%$ in this paper and increased with increased P . The estimated value was slightly larger than the exact value when σ_0 was relatively small. Otherwise, it was smaller than the exact value. However, it should be noted that the accuracy of the modified reference stress method was also dependent on the accuracy of the calculated σ_{ref} .

The accuracy of Eq. (4) is shown in Fig. 5. Cases 1–6 had the same P value and material properties though they had different values for σ_0 , which increased from 0 MPa to 150 MPa, respectively. As demonstrated by the stars in Fig. 5 for cases 1–6, the error decreased initially with increased σ_0 and reached a minimum value of -8% before increasing to -6%. The error was within $\pm 10\%$ for cases 1–6. Cases 4, 10, 11, and 12 had the same material properties with $\sigma_0 = 90$ MPa and P values ranging from 9000 N to 12,000 N, as shown by the solid circles in Fig. 5. Their errors increased from -6% to -3% with increased P . Therefore, the accuracy of Eq. (4) was possibly affected by σ_0 and P . Cases 1, 7, 8, and 9 had the same material properties with $\sigma_0 = 0$ MPa and P ranging from 9000 N to 12,000 N. Their errors changed from 6% to -5% and then to 6%, as indicated by the open circles in Fig. 5. The error was randomly distributed within $\pm 10\%$ for cases 1, 7, 8, and 9. The error was thus due

to the computational error produced by the Abaqus software for cases 1, 7, 8, and 9. Since the error range for cases 1, 7, 8, and 9 was similar to those for cases 2–6 and cases 10–12, the errors for cases 2–6 and cases 10–12 may also have been due to computational errors in the Abaqus software. Therefore, it was difficult to establish whether the accuracy of Eq. (4) was affected by P and σ_0 . Since the error was within $\pm 10\%$ and was possibly due to computational errors in the Abaqus software for cases 1–12, it could be concluded that the accuracy of Eq. (4) was sufficient, that the results were unaffected by σ_0 , and that the equation could be directly used to calculate C^* for power-law creep materials with threshold stress. The accuracy of Eq. (4) did not appear to be affected by σ_0 because the effect of σ_0 was calculated using the load line deflection rate, $(\dot{V}_c)_{SS}$.

Further research is necessary to obtain h_1 under various n , σ_0 , a/W , geometrical shapes, and loading conditions (plane strain and plane stress). The calculation equation of C^* in ASTM E 1457 can be directly used in lab conditions for power-law creep materials with threshold stress. The modified GE/EPRI method and the reference stress method can both be used to estimate C^* . The modified GE/EPRI method can be considered a conservative method, while the modified reference stress method can be considered an overestimated method with very large values of σ_0 when used to estimate the creep crack growth or predict the lifetime of high temperature components.

5. Conclusions

The GE/EPRI method and reference stress method were modified to estimate C^* for power-law creep material properties with threshold stress. Finite element analyses were performed to verify the accuracy of the modified methods. The accuracy of the calculation equation of C^* in ASTM E 1457 when used in power-law creep materials with threshold stress was investigated and the following conclusions were obtained:

- (1) The modified GE/EPRI method was sufficiently exact as an engineering method. h_1 was slightly affected by the applied load and significantly affected by the threshold stress. Additional studies are required to obtain h_1 under various threshold stress conditions for different creep exponents and geometrical shapes.
- (2) The accuracy of the modified reference stress method was within $\pm 40\%$ in this paper and increased slightly with an increase in the applied load.
- (3) The accuracy of the calculation equation of C^* in ASTM E 1457 was not affected by the threshold stress. Therefore, the equation could be directly used to calculate C^* for power-law creep materials with threshold stress.

Acknowledgments

This work was supported by the National Natural Science Foundation of China (51705078), Qishan Scholars Program of Fuzhou University in 2016 (XRC-1689), and Open Test Fund of Equipment of Fuzhou University in 2017 (2017T031).

References

- [1] Kumar V, German MD, Shih CF. An engineering approach for elastic-plastic fracture analysis. EPRI final report, NP-1931; 1981.
- [2] Kumar V, German MD. Elastic-plastic fracture analysis of through-wall and surface flaws in cylinders. EPRI report, NP-5596; 1988.
- [3] Goodall IW (editor). Reference stress methods: analysing safety and design. London: Professional Engineering Publishing; 2003.
- [4] Biglaria F, Nikbin KM, Goodall IW, Webster GA. Determination of fracture mechanics parameters J and C^* by finite element and reference stress methods for a semi-elliptical flaw in a plate. *Int J Pres Ves Pip* 2003;80:565–71.
- [5] Xuan FZ, Tu ST, Wang ZD. C^* estimation for cracks in mismatched welds and finite element validation. *Int J Fract* 2004;126:267–80.
- [6] Kim YJ, Huh NS, Kim YJ. Enhanced reference stress-based J and crack opening displacement estimation method for leak-before-break analysis and comparison with GE/EPRI method. *Fatigue Fract Eng M* 2001;24(4):243–54.
- [7] Kim YJ, Huh NS, Kim YJ. Estimations of creep fracture mechanics parameters for through-thickness cracked cylinders and finite element validation. *Fatigue Fract Eng M* 2003;26(3):229–44.
- [8] Tu ST. Creep behavior of crack near bi-material interface characterized by integral parameters. *Theor Appl Fract Mech* 2002;38:203–9.
- [9] Tu ST, Yoon KB. The influence of material mismatch on the evaluation of time-dependent fracture mechanics parameters. *Eng Fract Mech* 1999;64:765–80.
- [10] Gowhari-Anaraki AR, Djavanroodi F, Shadlou S. Estimation of C^* -integral in thin T-sections subjected to projection and remote loading base on elastic stress concentration factor. *Am J Appl Sci* 2008;5(5):586–96.
- [11] Gowhari-Anaraki AR, Djavanroodi F, Shadlou S. Estimation of C^* -integral for radial cracks in annular discs under constant angular velocity and internal pressure. *Am J Appl Sci* 2008;5(8):997–1004.
- [12] Xuan FZ, Tu ST, Wang ZD. A modification of ASTM E 1457 C^* estimation equation for compact tension specimen with a mismatched cross-weld. *Eng Fract Mech* 2005;72:2602–14.
- [13] Han BQ, Dunand DC. Creep of magnesium strengthened with high volume fractions of yttria dispersions. *Mater Sci Eng A-Struct* 2001;300(1–2):235–44.
- [14] Matsuda BN, Matsuura K. Creep behavior and threshold stress of an Al-Al₂O₃-Zr alloy. *Mater Trans* 1990;31(5):386–95.
- [15] Chen YX, Yan W, Wang W, Shan YY, Yang K. Constitutive equations of the minimum creep rate for 9% Cr heat resistant steels. *Mater Sci Eng A-Struct* 2012;534:649–53.
- [16] Yeh BYH, Nakashima H, Kurishita H, Goto S, Yoshinaga H. Threshold stress for high-temperature creep in particle strengthened Al-1.5 vol% Be alloys. *Mater Trans* 1990;31(4):284–92.
- [17] Ohji T, Kusunose T, Niihara K. Threshold stress in creep of alumina-silicon carbide nanocomposites. *J Am Ceram Soc* 1998;81(10):2713–6.
- [18] Cai B, Kong QP, Lu L, Lu K. Low temperature creep of nanocrystalline pure copper. *Mater Sci Eng A-Struct* 2000;286:188–92.
- [19] Saxena A. Nonlinear fracture mechanics for engineers. Florida: CRC Press LLC; 1998.
- [20] Kim YJ, Kim JS, Huh NS, Kim YJ. Engineering C^* -integral estimates for generalized creep behavior and finite element validation. *Int J Pres Ves Pip* 2002;79:427–43.

- [21] ASTM Standard. E1457-13: Standard test methods for measurement of creep crack growth times and rates in metals. ASTM; 2013.
- [22] Fernández R, Doncel GG. Threshold stress and load partitioning during creep of metal matrix composites. *Acta Mater* 2008;56:2549–62.
- [23] Shen JJ, Ikeda K, Hata S, Nakashima H. Creep mechanisms in a fine-grained Al-5356 alloy at low stress and high temperature. *Mater Trans* 2011;52(10):1890–8.
- [24] Lai HS, Yoon KB. Estimation of $C(t)$ and the creep crack tip stress field of functionally graded materials and verification via finite element analysis. *Compos Struct* 2016;153:728–37.
- [25] Lai HS, Ryu SW, Yoon KB, Lin XP. Estimation of C_t for weld cracks including HAZ softening region. *Mater High Temp* 2016;33(6):596–603.
- [26] Lai HS, Yoon KB. Study on the estimation of high temperature fracture parameter for mismatched weld creep cracks. *Eng Fract Mech* 2016;163:117–29.
- [27] Lai HS. Estimation of C_t of functionally graded materials under small scale creep stage. *Compos Struct* 2016;138:352–60.